



OPEN

DATA DESCRIPTOR

X-ray Coronary Angiogram images and SYNTAX score to develop Machine-Learning algorithms for CHD Diagnosis

Seyed Sajjad Mahmoudi^{1,8}, Mohammad Matin Alishani^{2,8}, Manijeh Emdadi³, Seyed Mahdi Hosseiniyan Khatibi⁴, Bahareh Khodaei⁵, Alireza Ghaffari⁶, Shahram Dabiri Oskui⁵, Samad Ghaffari⁷✉ & Saeed Pirmoradi⁵✉

Coronary Heart Disease (CHD) is becoming a leading cause of death worldwide. To assess coronary artery narrowing or stenosis, doctors use coronary angiography, which is considered the gold-standard method. Interventional cardiologists rely on angiography to decide on the best course of treatment for CHD, such as revascularization with bypass surgery, coronary stents, or medication. However, angiography has some issues, including operator bias, inter-observer variability, and poor reproducibility. The automated interpretation of coronary angiography is yet to be developed, and these tasks can only be performed by highly specialized physicians. Developing automated angiogram interpretation and coronary artery stenosis estimation using Artificial Intelligence (AI) approaches requires a large dataset of X-ray angiography images that include clinical information. We have collected 231 X-ray images of heart vessels, along with the necessary angiographic variables, including the SYNTAX score, to support the advancement of research on CHD-related machine learning and data mining algorithms. We hope that this dataset will ultimately contribute to advances in clinical diagnosis of CHD.

Background & Summary

Coronary Heart Disease (CHD) is an emerging cause of death in the world. In CHD, atherosclerotic plaques can limit blood flow to cardiac tissues by narrowing the coronary arteries^{1,2}. Coronary angiography is the gold-standard method to assess coronary artery narrowing³ or stenosis, which is minimally invasive and catheter-based. Also, interventional cardiologist utilizes it to make CHD treatment decisions. In the United States, interventional cardiologists perform over one million coronary angiograms yearly⁴. They rely on angiography to select worthy treatments, such as revascularization with bypass surgery, coronary stents, or CHD medication. In this process, the first step is the identification of artery stenosis with a severity of more than 70%³.

Visual estimation of coronary stenosis severity is the current standard method, which has remained unchanged for over 70 years⁵. It faces problems such as inter-observer variability, operator bias, and poor reproducibility⁶⁻¹⁰. Inter-observer variability rate of visual stenosis assessment changes from 15 to 45%^{7,11-13} and strongly depends on the operator's experience. Nearly 40% of interventional cardiologists perform less than 50 angiograms yearly, which is worrying statistics related to this issue¹⁴. These problems can lead to wrong CHD treatment, such as inappropriate coronary artery bypass surgery in 17% and using stents in 10% of patients⁷.

¹Department of Cardiology, School of Medicine, Urmia University of Medical Sciences, Urmia, Iran. ²Department of Computer Science, Faculty of Information Technology, Azarbaijan Shahid Madani University, Tabriz, Iran. ³Department of Computer Engineering, Abadan Branch, Islamic Azad University, Abadan, Iran. ⁴Rahat Breath and Sleep Research Center, Tabriz University of Medical Sciences, Tabriz, Iran. ⁵Clinical Research Development Unit of Tabriz Valiasr Hospital, Tabriz University of Medical Sciences, Tabriz, Iran. ⁶Faculty of Electrical and Computer Eng., University of Tabriz, Tabriz, Iran. ⁷Cardiovascular Research Center, Tabriz University of Medical Sciences, Tabriz, Iran. ⁸These authors contributed equally: Seyed Sajjad Mahmoudi, Mohammad Matin Alishani. ✉e-mail: ghafaris@gmail.com; said.pirmoradi@gmail.com

Therefore, developing new approaches to interpret angiograms and assess coronary stenosis more reproducible and standardized plays a critical role in clinical application.

Determining angiographic coronary stenosis severity is not fully automated by existing methods and needs significant operator input, which is rarely used in clinical applications². For this purpose, the existing approach is Quantitative Coronary Angiography (QCA). However, it requires manual effort by the interventional cardiologist, such as optimal frame selection within the angiogram video, identification of a reference object, and vessel wall tracing^{7,8,15}. These multiple-step manual efforts are time-consuming and restrict QCA primarily to research applications¹⁵. In addition, inter-observer variability in QCA measurements ranges from 10% to 30%¹⁶. Also, the SYNTAX score is another tool for risk stratification of patients undergoing percutaneous coronary intervention. It's based on 11 angiographic variables that provide a qualitative and quantitative characterization of coronary artery disease. The SYNTAX trial demonstrated that it is an effective tool for risk-stratifying patients with complex coronary artery disease undergoing percutaneous coronary intervention. Due to the several complex sequences of tasks in QCA/SYNTAX, full automation of coronary angiography interpretation has not been developed. These tasks are performed only via the expertise of highly sub-specialized physicians.

Developing automated angiogram interpretation and coronary artery stenosis estimation using Artificial Intelligence (AI) approaches needs datasets containing large amounts of X-ray angiography images with clinical information. Many studies have proposed AI-based methods for automated angiogram interpretation and coronary artery stenosis estimation in recent years. However, none of the datasets from the mentioned studies are available to other research groups, and there is no angiography image data with an associated SYNTAX score available. Collecting X-ray angiography images along with clinical information and interventional cardiologists' diagnoses for assessing coronary stenosis, and making this data publicly available, would be effective in advancing research and improving clinical outcomes. In the recent study, the authors collected excellent X-ray angiography images that highlight the use of deep learning algorithms for segmentation, which is extremely valuable¹⁷.

In this study, we have collected X-ray angiography images which include Two hundred thirty-two X-ray images of heart vessels. The dataset we have created includes the SYNTAX score and other angiographic variables necessary for calculating the SYNTAX score. Additionally, we have utilized Python libraries for the automated data reading process. We have also implemented a new algorithm to choose the best frames among multiple frames.

The data collected in this study is appropriate for classifying patients into risk groups based on the SYNTAX Score using machine learning algorithms. One of the strengths of this study is the detailed explanation of the SYNTAX calculation method and the table of information for each patient, which will be highly educational for training new specialists.

Methods

Ethical approval. This study was approved by the Ethics Committee of the Tabriz University of Medical Sciences, Tabriz, Iran (Ethical code: IR.TBZMED.REC.1402.518).

Patient Cohort. Two hundred thirty-one patients were randomly collected from the Shahid Madani Hospital Retrospectively, by a cardiologist in Tabriz, Iran, between February 2018 and 2020. X-ray angiography imaging of patients was performed, by an interventional cardiologist, in the Cath Lab of the hospital, and the images had acceptable quality for diagnosis. X-ray angiography images and clinical data were gathered from PACS (Picture Archiving and Communication System) and HIS (Hospital Information System) archives in retrospective form, respectively. The study was conducted by the principles of the Declaration of Helsinki (2013). Due to the retrospective nature of this study, a waiver of consent was granted and approved by the Human Research Ethics Committee of Tabriz University of Medical Sciences (Ethical Code: IR.TBZMED.REC.1402.518).

According to the Cath Lab report, all patients had a percentage of obstructive coronary artery stenosis of more than 70%. To determine the risk group of patients, the cardiologist calculated the SYNTAX score based on x-ray angiographic images. We reported statistical information related to x-ray angiographic images and clinical data based on SYNTAX score groups of patients.

Imaging. X-ray angiography imaging was acquired with Philips Allura Clarity (Philips, Amsterdam, Netherlands) and Siemens Axiom Artis (Siemens Healthineers, Germany) systems.

SYNTAX score Calculation. The open-source web-based software SYNTAX score calculator (version 2.28) was utilized to calculate the SYNTAX score of x-ray angiographic images that are available at the <https://syntaxscore.org/> web address. Also, cardiologists applied the open-source software MicroDicom (<https://www.microdicom.com/>) to display coronary artery images in the diagnosis process. The SYNTAX score calculator, an angiographic grading tool, is a set of points that add together to evaluate the complexity of coronary artery disease (CAD). Coronary trees with >50% diameter narrowing in vessels > 1.5 mm diameter are considered to determine these points¹⁸. The stenosis of 16 segments according to the AHA classification (see Fig. 1) was reported in this data for each sample and utilized for SYNTAX score calculation. For a more detailed understanding of the coronary tree segments, please refer to Table 1. Additionally, Table 2 provides a guide for calculating the SYNTAX score.

Frame Selection algorithm. The DICOM file for X-ray angiography contains numerous frames of the distinct view of the coronary artery. However, interventional cardiologists can observe the entire structure of the coronary artery in a specific position (as described in Table 4) with a low number of frames after the injection of a contrast agent. We require an automated tool that can select the best frames with a complete view of coronary arteries. This tool will be helpful for machine learning algorithms in diagnosing coronary artery disease.

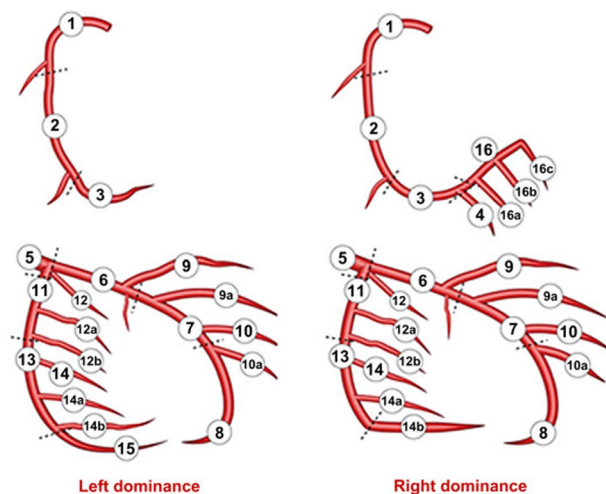


Fig. 1 Sixteen segments according to the AHA classification²¹.

Segment	Name	Segment Definition
1	RCA proximal	From ostium to and including the origin of the first RV branch.
2	RCA mid	RCA is immediately distal to the origin of the first RV branch to the acute margin of the heart.
3	RCA distal	From the acute margin of the heart to the origin of the posterior descending artery.
4	Right posterior descending	Originating from the distal coronary artery distal to the crux and running in the posterior interventricular groove.
16	Atrioventricular Continuation from RCA	Originating from the distal coronary artery distal to the crux and running in the atrioventricular groove.
16a	Posterolateral from RCA	First posterolateral branch from segment 16.
16b	Posterolateral from RCA	The second posterolateral branch from segment 16.
16c	Posterolateral from RCA	The third posterolateral branch from segment 16.
5	Left main	From the ostium of the LCA through bifurcation into left anterior descending and left circumflex branches.
6	LAD proximal	Proximal to and including the first major septal branch.
7	LAD mid	LAD is immediately distal to the origin of the first septal branch and extending to the point where LAD forms an angle (RAO view). If this angle is not identifiable, this segment ends at one-half the distance from the first septal to the apex of the heart, usually after two diagonal branches have originated.
8	LAD distal	The terminal portion of LAD begins at the end of the mid-segment and extends to or beyond the apex.
9	First diagonal	The first diagonal originates from segments 6 or 7.
9a	First diagonal a	Additional first diagonal originating from segment 6 or 7, before segment 8.
10	Second diagonal	The second diagonal originates from segment 8 or the transition between segments 7 and 8.
10a	Second diagonal a	Additional second diagonal originating from segment 8.
11	Proximal circumflex	The main stem of circumflex from its origin of the left main to and including the origin of the first obtuse marginal branch.
12	Ramus intermedius	The branch from trifurcating left main other than proximal LAD or LCX. Belongs to the circumflex territory.
12a	Obtuse marginal a	The first side branch of the circumflex running in general to the area of the obtuse margin of the heart (down and out in RAO view)
12b	Obtuse marginal b	The second additional branch of circumflex running in the same direction as 12.
13	Distal circumflex	The stem of the circumflex distal to the origin of the most distal obtuse marginal branch and running along the posterior left atrioventricular grooves. Caliber may be small or artery absent.
14	Left posterolateral	Running to the posterolateral surface of the left ventricle (horizontal and down in RAO view). May be absent or a division of an obtuse marginal branch.
14a	Left posterolateral a	Distal from 14 and running in the same direction.
14b	Left posterolateral b	Distal from 14, and 14a running in the same direction.
15	Left posterior descending	The most distal part of the dominant left circumflex when present. Gives origin to septal branches. When this artery is present, segment 4 is usually absent

Table 1. Definition of the coronary tree segments²³.

Steps	Variable assessed	Description
Step 1	Dominance	The weight of individual coronary segments varies according to coronary artery dominance (right or left). Co-dominance does not exist as an option in the SYNTAX score.
Step 2	Coronary segment	The diseased coronary segment directly affects the score as each coronary segment is assigned a weight depending on its location, ranging from 0.5 (i.e. the posterolateral branch) to 6 (i.e. left main in case of left dominance) ²⁴ .
Step 3	Diameter stenosis	The score of each diseased coronary segment is multiplied by two in case of stenosis 50–99% and by five in case of total occlusion. In case of total occlusion, additional points will be added as follows: <ul style="list-style-type: none"> • Age > 3 months or unknown: +1 • Blunt stump: +1 • Bridging: +1 • First segment visible distally: +1 per non-visible segment Side branch at the occlusion: <ul style="list-style-type: none"> +1 if <1.5 mm diameter +1 if both <1.5 mm and ≥1.5 mm diameter +0 if ≥1.5 mm diameter (i.e. bifurcation lesion)
Step 4	Trifurcation lesion	The presence of a trifurcation lesion adds additional points based on the number of diseased segments: <ul style="list-style-type: none"> • 1 segment +3 • 2 segments +4 • 3 segments +5 • 4 segments +6
Step 5	Bifurcation lesion	The presence of a bifurcation lesion adds additional points based on the type of bifurcation according to the Medina classification: <ul style="list-style-type: none"> • Medina 1,0,0–0,1,0–1,1,0 +1 • Medina 1,1,1–0,0,1–1,0,1–0,1,1 +2, Moreover, the presence of a bifurcation angle <70° adds one additional point
Step 6	Aorto-ostial lesion	The presence of aorto-ostial lesion segments adds one additional point
Step 7	Severe tortuosity	The presence of severe tortuosity proximal of the diseased segment adds two additional points
Step 8	Lesion length	Lesion length >20 mm adds one additional point
Step 9	Calcification	The presence of heavy calcification adds two additional points
Step 10	Thrombus	The presence of a thrombus adds one additional point
Step 11	Diffuse disease/ small vessels	The presence of diffusely diseased and narrowed segments distal to the lesion (i.e. when at least 75% of the length of the segment distal to the lesion has a vessel diameter <2 mm) adds one point per segment number

Table 2. Guide for calculating the SYNTAX score²⁴.

Additionally, it will assist us in providing a sufficient dataset of x-ray angiography images for the machine learning applications in this study.

In our study, we have introduced a tool that automatically selects frames using a Machine Learning algorithm. We utilized the mean structural similarity index (MSSIM) measure for this purpose. SSIM is a commonly used image similarity measure that has proven to be effective in assessing image quality in various applications¹⁹. We first transformed the DICOM file into multiple JPG files to obtain an image with a complete view of the coronary artery. Next, we calculated the Mean Structural Similarity Index (MSSIM) between the first frame (used as a reference) and the remaining frames. Then, we selected the three frames with the lowest MSSIM value, the whole frame selection process is shown in Fig. 2. MSSIM is calculated using Eq. 1.

$$MSSIM(X, Y) = \frac{1}{M} \sum_{j=1}^M SSIM(x_j, y_j) \quad (1)$$

In the MSSIM technique, we apply the SSIM metric to different regions of the image, instead of applying it globally to the entire image at once. This is done by dividing the X and Y input images into M sections, computing the SSIM for each section individually, and finally, calculating the mean SSIM value as the MSSIM of X and Y Images. The SSIM metric is a measure of similarity between two images, which can range from -1 (very different) to 1 (very similar or the same). These values are then normalized to be within the range of $[0, 1]$ ²⁰. SSIM is calculated using Eq. 2.

$$SSIM(X, Y) = l(X, Y)^\alpha c(X, Y)^\beta s(X, Y)^\gamma \quad (2)$$

In Eq. 2, the coefficients α , β , and γ have values greater than zero. The Structural Similarity Index (SSIM) has three essential properties, which are luminance, contrast, and structure comparing functions. Luminance, contrast, and structure comparing functions are determined using Eqs. 3 to 5.

$$l(X, Y) = \frac{2\mu_x\mu_y + c_1}{\mu_x^2 + \mu_y^2 + c_1} \quad (3)$$

$$c(X, Y) = \frac{2\sigma_x\sigma_y + c_2}{\sigma_x^2 + \sigma_y^2 + c_2} \quad (4)$$

Sample	\\ sample in “Patient ID-SYNTAX-info” file with K lesions
	<pre> {‘Patient ID’: ‘Dominance’: ‘Number of lesions’: ‘Lesion 1-Segment numbers involved’: ‘Lesion 1-Total occlusion’: ‘Lesion 1-Total occlusion segment numbers’: ‘Lesion 1-Most proximal segment number’: ‘Lesion 1-More than 3 months’: ‘Lesion 1-Blunt stump’: ‘Lesion 1-Bridging’: ‘Lesion 1-The first segment beyond the T.O. visualized by contrast’: ‘Lesion 1-Side branch’: ‘Lesion 1-Trifurcation’: ‘Lesion 1-Bifurcation’: ‘Lesion 1-Bifurcation angulation’: ‘Lesion 1-Aorto Ostial lesion’: ‘Lesion 1-Severe Tortuosity’: ‘Lesion 1-Length >20 mm’: ‘Lesion 1-Heavy calcification’: ‘Lesion 1-Thrombus’: . . . ‘Lesion K-Segment numbers involved’: ‘Lesion K-Total occlusion’: ‘Lesion K-Total occlusion segment numbers’: ‘Lesion K-Most proximal segment number’: ‘Lesion K-More than 3 months’: ‘Lesion K-Blunt stump’: ‘Lesion K-Bridging’: ‘Lesion K-The first segment beyond the T.O. visualized by contrast’: ‘Lesion K-Side branch’: ‘Lesion K-Trifurcation’: ‘Lesion K-Bifurcation’: ‘Lesion K-Bifurcation angulation’: ‘Lesion K-Aorto Ostial lesion’: ‘Lesion K-Severe Tortuosity’: ‘Lesion K-Length >20 mm’: ‘Lesion K-Heavy calcification’: ‘Lesion K-Thrombus’: ‘SYNTAX Score’: ‘Diffuse disease/Small vessels’:} </pre>

Table 3. Extracted information from the SYNTAX score report of the i^{th} patient²².

$$s(X, Y) = \frac{\sigma_{xy} + c_3}{\sigma_x \sigma_y + c_3} \quad (5)$$

μ_x , μ_y are average values and σ_x , σ_y are the standard deviations over all the pixel values of X and Y images. σ_{xy} is the covariance of the pixel values of X and Y images. To ensure that the denominator doesn't become zero, we use three constants c_1 , c_2 , and c_3 .

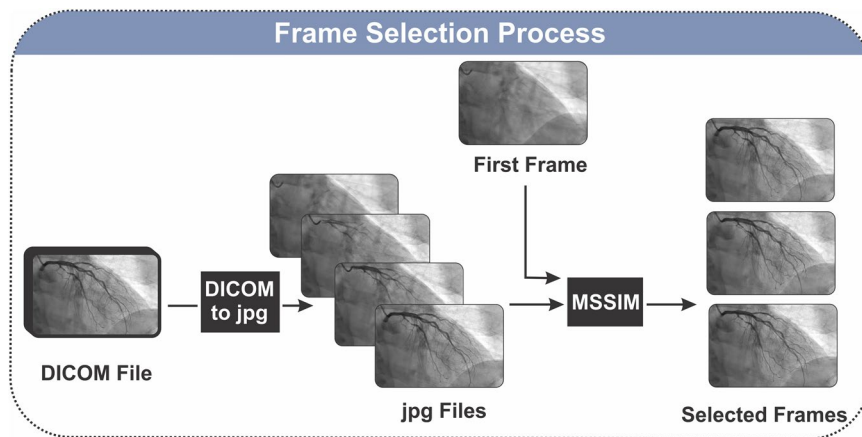


Fig. 2 The process of frame selection.

Projection	Definition
RAO Cranial	−45° to −15° RAO; 15° to 45° Cranial
AP Cranial	−15° to 15° AP; 15° to 45° Cranial
LAO Cranial	15° to 45° LAO; 15° to 45° Cranial
RAO Straight	−45° to −15° RAO; −15° to 15° AP
AP	−15° to 15° AP; −15° to 15° AP
RAO Caudal	−45° to −15° RAO; −45° to −15° Caudal
AP Caudal	−15° to 15° AP; −45° to −15° Caudal
LAO Caudal	15° to 45° LAO; −45° to −15° Caudal
LAO Straight	15° to 45° LAO; −15° to 15° AP
LAO Lateral	70° to 110° LAO; −15° to 15° AP
RAO Lateral	−110° to −70° RAO; −15° to 15° AP
Other	Any angles not belonging to the previous definitions

Table 4. Angiographic Projection Angle². **Abbreviations:** RAO: Right Anterior Oblique; AP: Antero-posterior; LAO: Left Anterior Oblique.

Data Records

Data description. We extracted patient information from the collected data, including x-ray angiography images in Dicom format and SYNTAX score reports in PDF format, and then applied Python libraries to process these files automatically, including Pandas, Numpy, Matplotlib, Seaborn, Scikit-Learn, Pickle, and PyPDF2 libraries. The extracted information from the SYNTAX score report was presented as “Patient ID-SYNTAX-info”, a dictionary python file in “.pkl” format. The structure of the “Patient ID-SYNTAX-info” is displayed in Table 3 in more detail, which is reported for each patient. Technical expressions in Tables 1, 2 are explained in <https://syntaxscore.org/> and M. Yadav *et al.* SYNTAX score reference paper²¹.

In the angiography process, interventional cardiologists take several series of X-ray images from various projections to diagnose accurately, and the number of series/projections depends on the cardiologist’s opinion. We automatically selected three frames from each series/projection based on the proposed algorithm, ensuring that the coronary tree segments were clearly recognizable in each projection. We applied Python libraries to automatically process DICOM files, including Pydicom, and Scikit-image libraries. The extracted frames were placed into a main folder with the patient ID name, and each series/projection was displayed in a subfolder with the projection symbol name. The description of standard projections is available in Table 4 in more detail. In angiography, various projections are utilized to visualize blood vessels and surrounding anatomical structures from different angles. These projections aid in identifying vascular abnormalities, guiding interventions, and assessing the spatial relationship of vessels. More information on key types of projections in angiography is available in the supplementary. The information extracted from the x-ray angiography images was presented as a dictionary Python file in “.pkl” format named “Patient ID-image-info”. The structure of the file is displayed in Table 5 for each patient. Finally, the image data of 231 patients including 1153 angiography views (total) and 3459 images (three images per view) were reported.

Data statistics. The SYNTAX score calculator reports the parameters for each sample based on the given questions displayed in Table 3. In this section, we visualized this information based on SYNTAX score risk groups as shown in Supplementary Figs. S1–S3. Risk groups are defined based on the SYNTAX score: low risk with $SYNTAX\ score \leq 22$, medium risk with $22 < SYNTAX\ score \leq 32$, and high risk with $SYNTAX\ score > 32$ ²¹. The purpose of Supplementary Figs S1–S3 was to provide information based on score calculations, categorized by risk groups, to give specialists a clear understanding of patient population distribution and risk groups for score calculation.

Sample	\\ sample in “Patient ID-image-info” file with K series or projection
	<pre> {‘Patient ID’: ‘SYNTAX Score’: ‘Dicom File 0’: { ‘Dicom Projection Info’: ‘Coronary Artery Segments Info’: \\ observable artery segments in this series or projection ‘Dicom Shape Info’: ‘Frames Index’: \\ selected frames index ‘Image 0’: \\ image matrix ‘Image 1’: ‘Image 2’: } ‘Dicom File 1’: { ‘Dicom Projection Info’: ‘Coronary Artery Segments Info’: ‘Dicom Shape Info’: ‘Frames Index’: ‘Image 0’: ‘Image 1’: ‘Image 2’: } . . . ‘Dicom File K’: { ‘Dicom Projection Info’: ‘Coronary Artery Segments Info’: ‘Dicom Shape Info’: ‘Frames Index’: ‘Image 0’: ‘Image 1’: ‘Image 2’: } } </pre>

Table 5. Extracted information from the x-ray angiography images of the i^{th} patient²².

Technical Validation

The dataset underwent technical validation using a three-tiered approach:

(1) Evaluation of X-ray angiography image quality by two interventional cardiologists with over 20 and 5 years of experience, respectively. (2) Assessment of SYNTAX score calculation reports by two interventional cardiologists. (3) Quality evaluation of selected X-ray angiography frames using machine learning approaches by two AI experts.

Data availability

All clinical data and x-ray angiography images are publicly available on the Figshare repository with “<https://doi.org/10.6084/m9.figshare.25801447>” DOI code²².

Code availability

The corresponding authors have provided the developed code for the frame selection process using a machine-learning approach, named “Frame Selection Function.py” on the Figshare repository with the DOI “<https://doi.org/10.6084/m9.figshare.25801447>”²². We used Python libraries, including the “sewar” library, to carry out the frame selection process. The mathematical concept is explained in the “Feature Selection Algorithm” section in greater detail. Ultimately, we employed the proposed algorithm to automatically select three frames in each series/projection. As a result, coronary tree segments were identifiable in that projection.

Received: 14 June 2024; Accepted: 28 February 2025;

Published online: 21 March 2025

References

1. Virani, S. S. *et al.* Heart disease and stroke statistics—2020 update: a report from the American Heart Association. *Circulation* **141**, e139–e596 (2020).
2. Avram, R. *et al.* CathAI: fully automated coronary angiography interpretation and stenosis estimation. *npj Digital Medicine* **6**, 142 (2023).
3. Patel, M. R. *et al.* ACC/AATS/AHA/ASE/ASNC/SCAI/SCCT/STS 2017 appropriate use criteria for coronary revascularization in patients with stable ischemic heart disease: a report of the American College of Cardiology appropriate use criteria task force, American Association for Thoracic Surgery, American Heart Association, American Society of Echocardiography, American Society of Nuclear Cardiology, Society for Cardiovascular Angiography and Interventions, Society of Cardiovascular Computed Tomography, and Society of Thoracic Surgeons. *Journal of the American College of Cardiology* **69**, 2212–2241 (2017).
4. Mozaffarian, D. *et al.*
5. Smith, S. C. Jr *et al.* ACC/AHA guidelines for percutaneous coronary intervention (revision of the 1993 PTCA guidelines)—executive summary: a report of the American College of Cardiology/American Heart Association task force on practice guidelines (Committee to revise the 1993 guidelines for percutaneous transluminal coronary angioplasty) endorsed by the Society for Cardiac Angiography and Interventions. *Circulation* **103**, 3019–3041 (2001).

6. Zir, L. M., Miller, S. W., Dinsmore, R. E., Gilbert, J. & Harthorne, J. Interobserver variability in coronary angiography. *Circulation* **53**, 627–632 (1976).
7. Leape, L. L. *et al.* Effect of variability in the interpretation of coronary angiograms on the appropriateness of use of coronary revascularization procedures. *American Heart Journal* **139**, 106–113 (2000).
8. Sirnes, P. A., Myreng, Y., Mølsted, P. & Golf, S. Reproducibility of quantitative coronary analysis: Assessment of variability due to frame selection, different observers, and different cinefilmless laboratories. *The International Journal of Cardiac Imaging* **12**, 197–203 (1996).
9. Zhang, H. *et al.* Comparison of physician visual assessment with quantitative coronary angiography in assessment of stenosis severity in China. *JAMA Internal Medicine* **178**, 239–247 (2018).
10. Nallamothu, B. K. *et al.* Comparison of clinical interpretation with visual assessment and quantitative coronary angiography in patients undergoing percutaneous coronary intervention in contemporary practice: the Assessing Angiography (A2) project. *Circulation* **127**, 1793–1800 (2013).
11. Marcus, M. L. *et al.* Visual estimates of percent diameter coronary stenosis: “a battered gold standard”. *Journal of the American College of Cardiology* **11**, 882–885 (1988).
12. Raphael, M. & Donaldson, R. A. “significant” stenosis: thirty years on. *The Lancet* **333**, 207–209 (1989).
13. Grundeken, M. J. *et al.* Inter-Core Lab Variability in Analyzing Quantitative Coronary Angiography for Bifurcation Lesions: A Post-Hoc Analysis of a Randomized Trial. *JACC: Cardiovascular Interventions* **8**, 305–314 (2015).
14. Harold, J. G. *et al.* ACCF/AHA/SCAI 2013 update of the clinical competence statement on coronary artery interventional procedures: a report of the American College of Cardiology Foundation/American Heart Association/American College of Physicians Task Force on Clinical Competence and Training (writing committee to revise the 2007 clinical competence statement on cardiac interventional procedures). *Circulation* **128**, 436–472 (2013).
15. Garrone, P. *et al.* Quantitative coronary angiography in the current era: principles and applications. *Journal of interventional cardiology* **22**, 527–536 (2009).
16. Keane, D. *et al.* Comparative validation of quantitative coronary angiography systems: results and implications from a multicenter study using a standardized approach. *Circulation* **91**, 2174–2183 (1995).
17. Popov, M. *et al.* Dataset for Automatic Region-based Coronary Artery Disease Diagnostics Using X-Ray Angiography Images. *Scientific Data* **11**, 20, <https://doi.org/10.1038/s41597-023-02871-z> (2024).
18. Lim, M. J., Zynda, T. K., Kern, M. J., Seto, A. H. & Suh, W. M. in *Interventional Cardiac Catheterization Handbook (Third Edition)* (ed Morton J. Kern) 220–243 (W.B. Saunders, 2013).
19. Nilsson, J. & Akenine-Möller, T. Understanding ssim. *arXiv preprint arXiv:2006.13846* (2020).
20. Wang, Z., Bovik, A. C., Sheikh, H. R. & Simoncelli, E. P. Image quality assessment: from error visibility to structural similarity. *IEEE transactions on image processing* **13**, 600–612 (2004).
21. Yadav, M. *et al.* Prediction of Coronary Risk by SYNTAX and Derived Scores: Synergy Between Percutaneous Coronary Intervention With Taxus and Cardiac Surgery. *Journal of the American College of Cardiology* **62**, 1219–1230, <https://doi.org/10.1016/j.jacc.2013.06.047> (2013).
22. Pirmoradi, S. in *X-Ray Angiography Images and SYNTAX-Score Dataset* (Figshare. Dataset. <https://doi.org/10.6084/m9.figshare.25801447.v1> 2024).
23. Kini, A., Sharma, S. K. & Narula, J. Practical manual of interventional cardiology. (Springer, 2014).
24. Neumann, F.-J. *et al.* 2018 ESC/EACTS Guidelines on myocardial revascularization. *European Heart Journal* **40**, 87–165, <https://doi.org/10.1093/eurheartj/ehy394> (2018).

Acknowledgements

This work was financially supported by the Iran National Science Foundation (INSF), Tehran, Iran (# 98028439) and the Clinical Research Development Unit of Tabriz Valiasr Hospital, Tabriz University of Medical Sciences, Tabriz, Iran (# 70953). Also, the authors would like to thank the Shahid Madani Hospital and the Clinical Research Development Unit of Tabriz Valiasr Hospital, Tabriz University of Medical Sciences, Tabriz, Iran for their assistance in this research.

Author contributions

Conception and design study: S.G. and S.P.; Data analysis: S.P., M.M.A., B.K., and S.S.M.; Writing original draft: S.P., M.E. and S.D.O.; Review and editing: all authors, Final Revision: S.P., A.G. and S.G.;

Competing interests

The authors declare no competing interests.

Additional information

Supplementary information The online version contains supplementary material available at <https://doi.org/10.1038/s41597-025-04727-0>.

Correspondence and requests for materials should be addressed to S.G. or S.P.

Reprints and permissions information is available at www.nature.com/reprints.

Publisher's note Springer Nature remains neutral with regard to jurisdictional claims in published maps and institutional affiliations.



Open Access This article is licensed under a Creative Commons Attribution-NonCommercial-NoDerivatives 4.0 International License, which permits any non-commercial use, sharing, distribution and reproduction in any medium or format, as long as you give appropriate credit to the original author(s) and the source, provide a link to the Creative Commons licence, and indicate if you modified the licensed material. You do not have permission under this licence to share adapted material derived from this article or parts of it. The images or other third party material in this article are included in the article's Creative Commons licence, unless indicated otherwise in a credit line to the material. If material is not included in the article's Creative Commons licence and your intended use is not permitted by statutory regulation or exceeds the permitted use, you will need to obtain permission directly from the copyright holder. To view a copy of this licence, visit <http://creativecommons.org/licenses/by-nc-nd/4.0/>.

© The Author(s) 2025